

Competition between Spin Echo and Spin Self-Rephasing in a Trapped Atom Interferometer

C. Solaro,¹ A. Bonnin,¹ F. Combes,² M. Lopez,¹ X. Alauze,¹ J.-N. Fuchs,^{2,3} F. Piéchon,² and F. Pereira Dos Santos^{1,*}

¹*SYRTE, Observatoire de Paris, PSL Research University,
CNRS, Sorbonne Universités, UPMC Univ. Paris 06, LNE,
61 Avenue de l'Observatoire, 75014 Paris, France*

²*Laboratoire de Physique des Solides, CNRS UMR 8502, Univ. Paris-Sud, Université Paris-Saclay
F-91405 Orsay CEDEX, France*

³*Laboratoire de Physique Théorique de la Matière Condensée,
CNRS UMR 7600, Univ. Pierre et Marie Curie,
4 place Jussieu, 75252 Paris CEDEX 05, France*

(Dated: June 6, 2025)

We perform Ramsey interferometry on an ultracold ^{87}Rb ensemble confined in an optical dipole trap. We use a π -pulse set at the middle of the interferometer to restore the coherence of the spin ensemble by canceling out phase inhomogeneities and creating a spin echo in the contrast. However, for high atomic densities, we observe the opposite behavior: the π -pulse accelerates the dephasing of the spin ensemble leading to a faster contrast decay of the interferometer. We understand this phenomenon as a competition between the spin-echo technique and an exchange-interaction driven spin self-rephasing mechanism based on the identical spin rotation effect (ISRE). Our experimental data is well reproduced by a numerical model.

PACS numbers: 05.30.-d, 37.25.+k, 32.80.Qk, 67.85.-d

A long coherence time is crucial for the coherent manipulation of quantum systems. In quantum computing, high-precision spectroscopy as well as in atom interferometry, preventing pure quantum states from decaying into a statistical mixture is challenging. In particular, when manipulating trapped ensembles, particles experience different trapping potentials and their spins precess at different rates creating a deleterious dephasing of coherences. Several techniques have been developed to overcome this limitation and to extend the coherence of the spin ensemble. The use of a magic wavelength for optically trapped atomic clouds [1, 2], the addition of a compensating field [3] or the mutual compensation scheme in magnetically trapped Rb ensemble [4] have been demonstrated. All such techniques, however, only reduce the dephasing that is slowed down but never cancelled.

A widespread technique that cancels out inhomogeneous dephasing is to create a spin echo via a π -pulse as originally thought of for RMN spectroscopy [5] and later on extended to cold gases [6]. The spin-echo technique reverses the inhomogeneous dephasing of a spin ensemble, which significantly increases the coherence time of the quantum system. Especially, inertial atomic sensors highly benefit from spin-echo techniques as, for symmetric interferometers, it cancels out unwanted clock effects [7], enabling unprecedented high sensitivities on the measurement of inertial forces [8–13]. In such configurations, however, dephasing sources originating from atom transverse motion [14, 15] can only be tackled by cooling the particles to lower temperatures, suggesting the use of

dense ultracold gases. Yet, in such a regime, collisional processes can also lead to inhomogeneous broadening and decoherence of the spin ensemble [16]. The spin-echo technique can in principle just as well cancel out mean-field shift inhomogeneities which is expected to restore the coherence of a spin ensemble at low temperatures.

However, using Ramsey interferometry and the spin-echo technique on an ultracold ^{87}Rb ensemble confined in an optical dipole trap, we observe the opposite behavior: applying a π -pulse in the middle of the Ramsey sequence increases spin dephasing leading to a faster loss of coherence of the spin ensemble. This unexpected phenomenon results from the interplay between the π -pulse and a collective spin self-rephasing (SSR) mechanism [17] which is due to the cumulative effect of the identical spin rotation effect (ISRE) in a trapped collisionless gas. Originating from atomic interactions and indistinguishability, ISRE is responsible for the exchange mean-field [18] and is characterized by the exchange rate $\omega_{ex} = 4\pi\hbar a_{12}\bar{n}/m$, where a_{12} is the relevant scattering length [19], \bar{n} the mean atomic density and m the atomic mass. In this Letter, we investigate the interplay between the widely used spin-echo technique and SSR, two different rephasing mechanisms that, surprisingly, do not collaborate.

Experimental set-up - In our system, we manipulate laser-cooled ultracold ^{87}Rb atoms trapped in a 3D optical dipole trap red-detuned far from resonance ($\lambda = 1070$ nm). The trap consists of two intersecting beams of 30 and $176\text{ }\mu\text{m}$ waists with maximum powers of 6 and 45 W respectively. After loading the trap from a magneto optical trap (MOT), we perform 2 s evaporative cooling to reach a cloud temperature of $T \sim 500$ nK with trap frequencies $\{\omega_1, \omega_2, \omega_3\} = 2\pi \times \{27, 279, 269\}$ Hz. With \bar{n} in the range of 10^{12} at/cm³, we explore the non-degenerate and collisionless (Knudsen) regime

* franck.pereira@obspm.fr

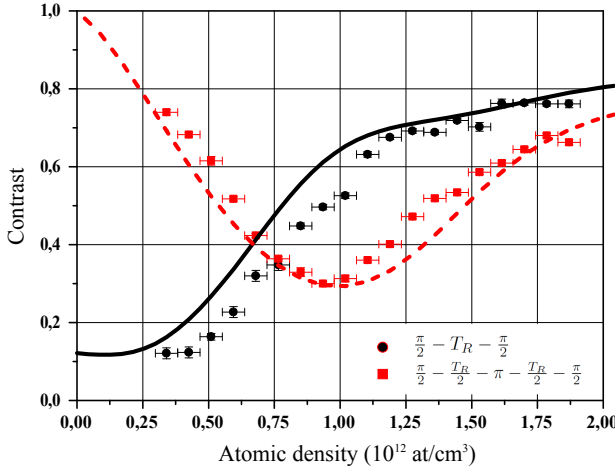


FIG. 1. (color online). Ramsey fringe contrast as a function of the mean atomic density \bar{n} at a fixed Ramsey time $T_R = 0.4$ s. Red squares and black dots correspond to a Ramsey sequence with and without applying a π -pulse at $t_\pi = T_R/2$ respectively. Dashed red and solid black curves correspond to our simulation results. Black curve and dots: the contrast increases with the atomic density which is characteristic of the collective spin self-rephasing mechanism [17]. Red dashed curve and squares: the π -pulse is expected to help canceling out the inhomogeneous broadening leading to a much higher contrast. Surprisingly for densities larger than 0.75×10^{12} at/cm³, the π -pulse leads to a lower contrast which reaches a minimum at an intermediate density 1×10^{12} at/cm³. This non-monotonic behavior suggests a competition between spin echo and spin self-rephasing mechanisms.

where the trap frequencies are much larger than the rate γ_c of lateral collisions. These collisions are velocity changing elastic collisions, also known to be responsible for collisional narrowing [20]. The rate γ_c is given by $\sim 4\pi a^2 v_T \bar{n}$, where a is the scattering length [21] and $v_T = \sqrt{k_B T/m}$ the thermal velocity of the atoms. In our range of densities, γ_c remains lower than 5 s^{-1} . In order to maximize the contrast of our interferometers, while preserving highest atomic densities, the atoms are carefully polarized into the state $|5s^2 S_{1/2}, F = 1, m_F = 0\rangle$ to avoid spin relaxation [22] and to minimize their sensitivity to parasitic magnetic fields. During the early stage of evaporation, after switching on our quantification axis, a σ -polarized resonant pulse on the $|5s^2 S_{1/2}, F = 1\rangle$ to $|5s^2 P_{3/2}, F' = 0\rangle$ transition pumps 70% of the atoms into the dark state $|F = 1, m_F = 0\rangle$. A combination of microwave and optical pulses is then used after the evaporation to purify the atomic sample leading to a highly polarized spin ensemble where $98 \pm 1\%$ of the atoms are in the $|F = 1, m_F = 0\rangle$ state. After this preparation sequence, we use resonant microwave field on the $|F = 1, m_F = 0\rangle$ to $|F = 2, m_F = 0\rangle$ transition and perform Ramsey interferometry. We can implement a standard Ramsey interferometer RI ($\pi/2 - T_R - \pi/2$) or add a π -pulse in the interferometric sequence ($\pi/2 - t_\pi - \pi - t_2 - \pi/2$) with $T_R = t_\pi + t_2$. In particular we can realize a Ramsey

symmetric interferometer RSI when $t_2 = t_\pi$. After the interferometer, the atoms are released from the trap. Following a fall distance of about 15 cm, the populations in the two hyperfine states are measured. This state selective detection is based on fluorescence in horizontal light sheets at the bottom of the vacuum chamber [23]. Since this detection system does not resolve the different m_F states, $|F = 2, m_F = \pm 1\rangle$ states that are created during the interferometer sequence by spin relaxation contribute as a background, which reduces the contrast by about 15 % for $T_R = 1$ s and $\bar{n} = 2 \times 10^{12}$ at/cm³.

First Experiment - To illustrate the effect of the spin-echo technique and SSR onto the coherence of the spin ensemble, we display in figure 1 measurements of the Ramsey contrast with and without a π -pulse for different mean atomic densities \bar{n} . To vary \bar{n} , we vary the number of atoms by changing the MOT loading time, accessing densities from 0.3 to 2×10^{12} at/cm³ which modulate $\omega_{ex}/2\pi = 7.5 \times \bar{n}$ Hz with \bar{n} in units of $\times 10^{12}$ at/cm³. The cloud temperature was verified to remain constant within 15%. In this regime, inhomogeneous dephasing originates both from differential light shift induced by the trapping lasers and from mean-field interactions, and has for characteristic inhomogeneity $\Delta_0/2\pi = k_B T/2h \times \delta\alpha/\alpha + 2\sqrt{2}\hbar(a_{11} - a_{22})\bar{n}/m$ using the same definition of Δ_0 as in [17, 24]. Here $\delta\alpha$ and α are the differential and the total light shift per intensity. With $\delta\alpha/\alpha = 5.93 \times 10^{-5}$ and a_{11}, a_{22} the relevant scattering lengths [19] we have $\Delta_0/2\pi \approx 0.3 + 0.7\bar{n}$ Hz with \bar{n} in 10^{12} at/cm³. The Ramsey time is $T_R = 2t_\pi = 0.4$ s and the Ramsey fringe contrast is deduced by scanning the phase of the exciting field. Without any π -pulse, the contrast increases with the atomic density (figure 1 black dots), revealing the efficiency of the SSR mechanism. Applying a π -pulse is expected to help canceling out the inhomogeneous broadening, thus leading to a much higher contrast. For densities between 0.3 and 0.75×10^{12} at/cm³ the π -pulse indeed increases the contrast with respect to a RI, but its efficiency is diminished as the density increases (figure 1 red squares). In fact, for higher densities the π -pulse actually accelerates the dephasing, but in a non-monotonic manner so that the contrast reaches a minimum at an intermediate density 1×10^{12} at/cm³ and then substantially recovers at highest densities. This behavior traduces an unexpected competition between the individual spin echo and the collective SSR mechanisms.

Two macropins model - SSR was first observed in a magnetically trapped ^{87}Rb ensemble [17] and subsequently employed in an optical trap [24] to extend the coherence time of a spin ensemble. This noteworthy collective mechanism extends the coherence time up to several seconds and leads to revivals of the contrast at periods of the ISRE: $T_{ex} = 2\pi/\omega_{ex}$. Following the two macropins model of [25] gives a clear understanding of the interplay between SSR and the spin-echo technique. For that purpose, we divide the atomic population into two groups of equal size, each characterized by a macropin and

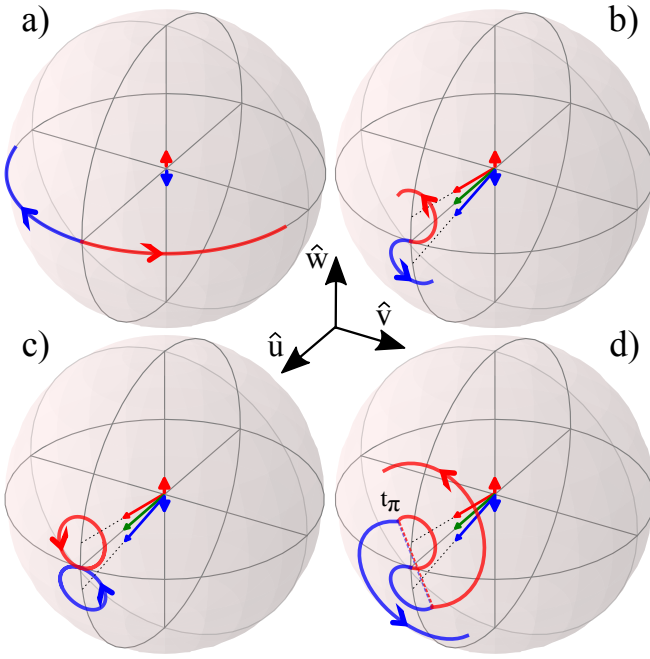


FIG. 2. (color online). The atomic population is divided into two equal classes of hot (red) and cold (blue) atoms that are represented by their macrospins trajectories on the Bloch sphere. (a) Inhomogeneous dephasing acts as a torque pointing in the \hat{w} direction that is of opposite sign for the two classes of atoms (red and blue short arrows). Hence the hot (cold) macrospin precesses towards the right (left). (b) With the ISRE, the effective magnetic field seen by the atoms is the sum of the inhomogeneity and the exchange mean-field proportional to the total spin (green arrow). As a consequence, the hot and cold macrospins precess around their effective magnetic fields (red and blue long arrows), so that if no π -pulse is applied they rephase at time T_{ex} : this is the SSR (c). If one applies a π -pulse when the two macrospins are out of the equatorial plane (u, v), the rephasing is degraded (d).

represent them by their trajectory on the Bloch sphere [17, 26]. The fast (slow) macrospin corresponds to the hot (cold) atoms which occupy higher (lower) transverse states of the 3D harmonic oscillator. For the sake of simplicity, we consider the dynamics in the rotating frame where the total spin always points in the \hat{u} direction of the Bloch sphere, and the π -pulses are rotations of π around this axis. Without the ISRE, the effective magnetic field seen by the macrospins only consists in the inhomogeneity which points along \hat{w} and in opposite directions for the two macrospins when working in the rotating frame. Hence the fast macrospin rotates towards the right while the slow macrospin rotates towards the left (figure 2(a)). Applying a π -pulse at time t_π would swap the two macrospins, so that at time $2t_\pi$ the macrospins would resynchronize leading to a spin echo (not shown). With the ISRE, the effective magnetic field is now the sum of the inhomogeneity and the exchange mean-field which is proportional to the total spin. As a consequence the fast macrospin rotates around this effective magnetic

field displayed as the long red arrow in figure 2(b), staying in the upper hemisphere of the Bloch sphere, while the slow macrospin evolves in the lower hemisphere. If no π -pulse is applied, the macrospins reach the equatorial plane again in their initial direction \hat{u} at the exchange period: the synchronization is perfect (figure 2(c)). However, if a π -pulse is applied, swapping the two macrospins positions, their trajectories are not confined to the upper (lower) hemisphere anymore (figure 2(d)), so that when they reach the equatorial plane again, they are not aligned: synchronization still occurs but is not perfect anymore. The effect of the π -pulse on SSR depends on the ratio between t_π and T_{ex} : when the macrospins are back in the equatorial plane the π -pulse has no effect ($t_\pi = pT_{ex}$ with $p \in \mathbb{N}$), while the effect is worst when the macrospins are maximally out of the equatorial plane ($t_\pi = (p + \frac{1}{2})T_{ex}$).

Second Experiment - To further investigate the competition between spin echo and SSR, we performed Ramsey interferometry with and without a π -pulse by scanning both the phase and the Ramsey time T_R from 0 to 900 ms. We extract the fringe contrast as a function of time for different atomic densities $\bar{n} = \{0.4, 0.9, 1.7, 2\} \times 10^{12}$ at/cm³ (figure 3). Black circles correspond to RIs and are similar to the ones in [17] whereas the red triangles correspond to RSI sequences with $t_2 = t_\pi = T_R/2$. For the lowest density, inhomogeneous broadening results in a $1/e$ dephasing time of $T_2^* \approx 0.2$ s corresponding to an inhomogeneity of $\Delta_0 \approx 1/T_2^* \approx 2\pi \times 0.8$ Hz using the same notations as [27], and agrees within 15% of our estimated inhomogeneity. In this regime we verify that the spin-echo technique is very efficient resulting in a $1/e$ coherence time of $T_2' = 0.8$ s (figure 3(a)). For the highest density, one observes a revival of the RI contrast at 0.25 s that also corresponds to a local minimum of the RSI contrast (figure 3(d)). Such a behavior is what one would expect from the two macrospins model described above. For the RI the spins are fully resynchronized at the exchange period T_{ex} resulting in a revival of the Ramsey contrast at $T_R = 0.25$ s. For the RSI, for the same Ramsey time, the atoms were swapped by a π -pulse at $t_\pi = T_R/2 = 0.125$ s (i.e. at half the exchange period) resulting into an acceleration of the dephasing and the lowest contrast of the interferometer. We observe that the same phenomenon occurs for different mean atomic densities $\bar{n} = \{2, 1.7, 0.9\} \times 10^{12}$ at/cm³ at different Ramsey time $T_0 \approx \{0.25, 0.32, 0.5\}$ s with about the same scaling $\bar{n}T_0 \approx cst$. Notice that no such other modulation is clearly observed at multiples $p \neq 1$ of the exchange period as it is expected from our simple model. This can be explained by our relatively high rate of lateral collisions γ_C that perturb SSR, resulting in a damping of the contrast revivals.

Many spins calculation - For a more quantitative understanding of this interplay between SSR and the spin-echo technique, we use the same model as in [17]. The trap is approximated by a 3D harmonic oscillator and the motion in the trap is treated semiclassically. Averag-

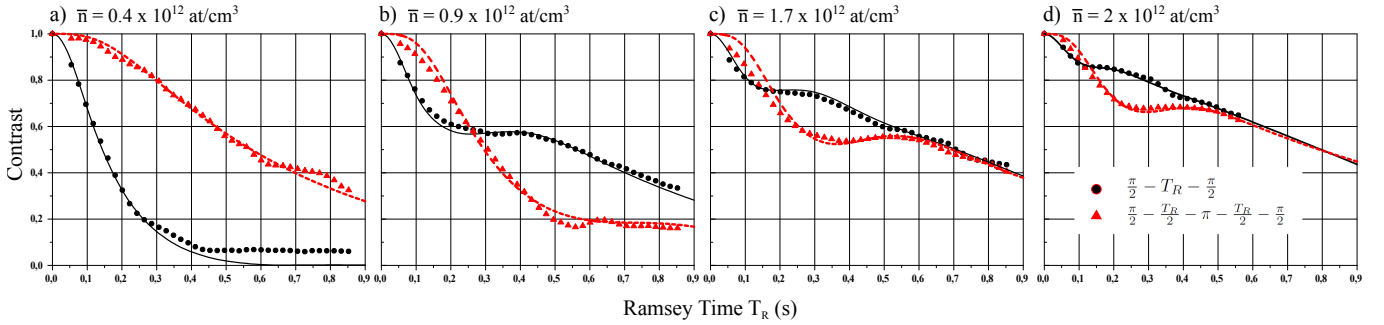


FIG. 3. (color online) Ramsey contrast versus Ramsey time T_R for RI (black dots) and RSI with $t_\pi = T_R/2$ (red triangles) for different mean atomic densities. Solid black and red dashed lines correspond to numerical simulations.

ing over the fast orbital motion in the trap leads to the following equation for an energy-isotropic spin density $\mathbf{S}(E, t)$ [17]:

$$\partial_t \mathbf{S}(E, t) \approx [\Delta_0 E \hat{\mathbf{w}} + \omega_{ex} \bar{\mathbf{S}}(t)] \times \mathbf{S}(E, t) - \gamma_c [\mathbf{S}(E, t) - \bar{\mathbf{S}}(t)]$$

with $\bar{\mathbf{S}}$ being the average spin:

$$\bar{\mathbf{S}}(t) = \int_0^\infty dE' \frac{E'^2}{2} e^{-E'} \mathbf{S}(E', t)$$

and $E \geq 0$ the motional energy in units of $k_B T$. The contrast is given by $C(t) = |\bar{\mathbf{S}}(t)|$. The two terms in the first bracket are the inhomogeneity that is linear in E for a harmonic oscillator, and the exchange mean-field in the infinite-range approximation. The second bracket is a relaxation term due to lateral collisions. The initial state is taken to be $\mathbf{S}(E, 0) = \hat{\mathbf{u}}$ immediately after the first $\pi/2$ -pulse. By adjusting the three parameters Δ_0 , ω_{ex} , γ_c with the simulation, we find good agreement with the experimental data (see curves on all figures). With respect to theoretical predictions, we find correction factors slightly different from [17] and [24]. Best fits are found for correction factors of 0.3 on ω_{ex} originating from the infinite-range approximation, and 0.3 on γ_c . Δ_0 agrees within 25% of the expected inhomogeneity.

Third Experiment - To further understand the spin dynamics and test our numerical model, we measured the evolution of the contrast after a fixed π -pulse for three different mean atomic densities $\bar{n} = \{0.4, 1.1, 1.7\} \times 10^{12}$ at/cm³ (figure 4). The π -pulse is applied at a time $t_\pi = 0.125$ s, we measured the contrast for different Ramsey times T_R between 0 and 500 ms (with t_2 not necessarily equal to t_π) in order to observe the formation of a spin echo. For the lowest density, we observe a net revival of the contrast at $T_R = 2t_\pi = 0.25$ s. As it is expected when exchange interactions and thus SSR are negligible, the π -pulse reverses the inhomogeneous dephasing and leads to a spin echo. For $\bar{n} = 1.1 \times 10^{12}$ at/cm³, a smaller echo occurs at a time $T_R \approx 0.18$ s < $2t_\pi$. This behavior is well reproduced by our model and is a consequence of SSR which tends to faster resynchronize the spins after the π -pulse. Increasing further the density, one can not see any echo since for such densities the π -pulse is now only a

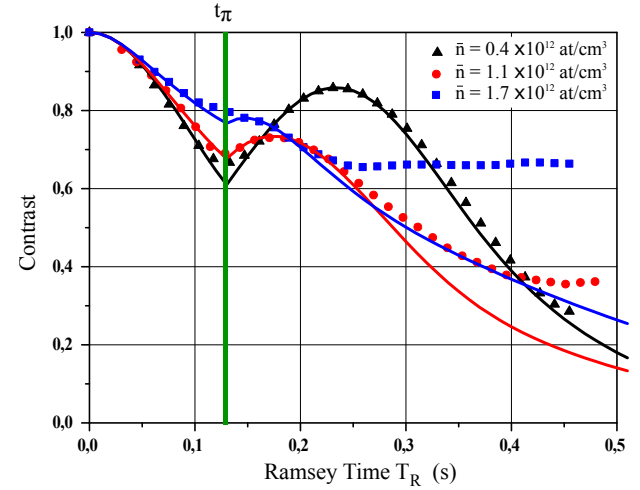


FIG. 4. (color online) Ramsey contrast versus Ramsey time T_R with a fixed π -pulse at $t_\pi = 125$ ms (green vertical line). Black triangles, red dots and blue squares correspond to the experimental data for different mean atomic densities. Black, red and blue lines correspond to numerical simulations.

small perturbation of SSR. For Ramsey times longer than $2t_\pi$ and for high atomic densities, we observe experimentally a plateau in the contrast that is not reproduced by our model (see blue squares in figure 4). We verified that neither atom loss nor spin relaxation could lead to such a plateau. This remains to be explained.

In summary, the interplay between spin-echo technique and spin self-rephasing mechanism was investigated both experimentally and theoretically. Our numerical simulations show good agreement with the experimental behaviors. We also proposed a simple two macrospins model to give a qualitative insight into this complex competition. Spin echoes have been used in a recent work [28] to observe the effect of the ISRE onto the spin diffusion coefficient of a unitary degenerate gas, allowing for the determination of the Leggett-Rice parameter [29]. Notice that in such a study, by contrast to our situation, SSR is absent as the gas is in the hydrodynamic rather than collisionless regime. Whereas the spin-echo technique is not used in standard Ramsey microwave interferometry

for clock spectroscopy and frequency measurements, it is widely used in other interferometer configurations as for example for the measurement of inertial forces, where π -pulses are used to cancel out all clocks effects. However, in such interferometers, the two partial wavepackets associated to the two internal states do not overlap perfectly and ISRE is expected to be weaker. The dependance of SSR with this overlap can be studied in an interferometer using atoms trapped in a lattice, such as [30].

ACKNOWLEDGMENTS

We thank Peter Rosenbusch, Wilfried Maineult and Kurt Gibble for useful discussions. We also acknowledge financial support by the IDEX PSL (ANR-10-IDEX-0001-02 PSL) and ANR (ANR-13-BS04-0003-01). A.B. thanks the Labex First-TF for financial support.

[1] H. Katori, M. Takamoto, V. G. Palchikov, and V. D. Ovsiannikov, *Physical Review Letters* **91**, 173005 (2003).

[2] H. Katori, K. Hashiguchi, E. Y. Ilinova, and V. D. Ovsiannikov, *Physical Review Letters* **103**, 153004 (2009).

[3] A. Kaplan, M. Fredslund Andersen, and N. Davidson, *Physical Review A* **66**, 045401 (2002).

[4] H. J. Lewandowski, D. M. Harber, D. L. Whitaker, and E. A. Cornell, *Physical Review Letters* **88**, 070403 (2002).

[5] E. L. Hahn, *Physical Review* **80**, 580 (1950).

[6] M. F. Andersen, A. Kaplan, and N. Davidson, *Physical Review Letters* **90**, 023001 (2003).

[7] M. Kasevich and S. Chu, *Physical Review Letters* **67**, 181 (1991).

[8] I. Dutta, D. Savoie, B. Fang, B. Venon, C. G. Alzar, R. Geiger, and A. Landragin, *Phys. Rev. Lett.* **116**, 183003 (2016).

[9] C. Freier, M. Hauth, V. Schkolnik, B. Leykauf, M. Schilling, H. Wziontek, H.-G. Scherneck, J. Mller, and A. Peters, (2015), arXiv:1512.05660.

[10] P. Gillot, O. Francis, A. Landragin, F. P. D. Santos, and S. Merlet, *Metrologia* **51**, L15 (2014).

[11] Z.-K. Hu, B.-L. Sun, X.-C. Duan, M.-K. Zhou, L.-L. Chen, S. Zhan, Q.-Z. Zhang, and J. Luo, *Phys. Rev. A* **88**, 043610 (2013).

[12] F. Sorrentino, Q. Bodart, L. Cacciapuoti, Y.-H. Lien, M. Prevedelli, G. Rosi, L. Salvi, and G. M. Tino, *Phys. Rev. A* **89**, 023607 (2014).

[13] G. W. Biedermann, X. Wu, L. Deslauriers, S. Roy, C. Mahareshwaraswamy, and M. A. Kasevich, *Phys. Rev. A* **91**, 033629 (2015).

[14] A. Louchet-Chauvet, T. Farah, Q. Bodart, A. Clairon, A. Landragin, S. Merlet, and F. P. D. Santos, *New Journal of Physics* **13**, 065025 (2011).

[15] A. Hilico, C. Solaro, M.-K. Zhou, M. Lopez, and F. Pereira dos Santos, *Physical Review A* **91**, 053616 (2015).

[16] D. M. Harber, H. J. Lewandowski, J. M. McGuirk, and E. A. Cornell, *Phys. Rev. A* **66**, 053616 (2002).

[17] C. Deutsch, F. Ramirez-Martinez, C. Lacroûte, F. Reinhard, T. Schneider, J. N. Fuchs, F. Piéchon, F. Laloë, J. Reichel, and P. Rosenbusch, *Physical Review Letters* **105**, 020401 (2010).

[18] C. Lhuillier and F. Laloë, *Journal de Physique* **43**, 197 (1982).

[19] We use $a_{11} = 101.284a_0$, $a_{22} = 94.946a_0$ and $a_{12} = 99.427a_0$ as calculated by C. Williams and found in Y. R. P. Sortais, *Construction d'une fontaine double à atomes froids de ^{87}Rb et ^{133}Cs ; Etude des effets dépendant du nombre d'atomes dans une fontaine*, PhD Thesis, Université Pierre et Marie Curie - Paris VI (2001).

[20] Y. Sagi, I. Almog, and N. Davidson, *Phys. Rev. Lett.* **105**, 093001 (2010).

[21] This expression for γ_c assumes $a_{11} \approx a_{22} \approx a_{12} \approx 100a_0 \approx a$ as for ^{87}Rb .

[22] A. Widera, F. Gerbier, S. Fölling, T. Gericke, O. Mandel, and I. Bloch, *Phys. Rev. Lett.* **95**, 190405 (2005).

[23] A. Clairon, P. Laurent, G. Santarelli, S. Ghezali, S. Lea, and M. Bahoura, *IEEE Trans. Instrum. Meas.* **44**, 128 (1995).

[24] G. Kleine Büning, J. Will, W. Ertmer, E. Rasel, J. Arlt, C. Klempf, F. Ramirez-Martinez, F. Piéchon, and P. Rosenbusch, *Physical Review Letters* **106**, 240801 (2011).

[25] F. Piéchon, J. N. Fuchs, and F. Laloë, *Physical Review Letters* **102**, 215301 (2009).

[26] K. Gibble, *Physics* **3**, 55 (2010).

[27] S. Kuhr, W. Alt, D. Schrader, I. Dotsenko, Y. Miroshnychenko, A. Rauschenbeutel, and D. Meschede, *Physical Review A* **72**, 023406 (2005).

[28] S. Trotzky, S. Beattie, C. Luciuk, S. Smale, A. B. Bardon, T. Enss, E. Taylor, S. Zhang, and J. H. Thywissen, *Phys. Rev. Lett.* **114**, 015301 (2015).

[29] A. J. Leggett and M. J. Rice, *Phys. Rev. Lett.* **20**, 586 (1968).

[30] B. Pelle, A. Hilico, G. Tackmann, Q. Beaufils, and F. Pereira dos Santos, *Phys. Rev. A* **87**, 023601 (2013).